Contribution from the Baker Laboratory of Chemistry,
Cornell University, Ithaca, New York 14853

Energy Density of Electronic States in Rare-Earth Molybdenum Chalcogenides As Deduced from Studies of Chemical Substitution Effects on Superconductivity

JEAN-MARIE TARASCON, DAVID C. JOHNSON, and M. J. SIENKO*

Received January 31, 1983

The pseudobinary systems $YbMo_6S_8$–$LaMo_6S_8$ and $YbMo_6Se_8$–$LaMo_6Se_8$ have been investigated to trace out the effect of replacing a two-electron donor, ytterbium, by a three-electron donor, lanthanum, on the crystal structure parameters and on the superconducting critical temperatures. The effect of selenium-for-sulfur replacement in the system $LaMo_6S_8$–$LaMo_6Se_8$ has been similarly explored. The results are used to derive quantitative information about the effect of unit-cell volume and of electron donation on the shape of the density-of-states curve. It is evident that a rigid-band model does not hold. Selenium-for-sulfur replacement, as expected, narrows the d-orbital-derived conduction band. Apparently $LaMo_6Se_8$ lies at the upper van Hove singularity, whereas $YbMo_6Se_8$ falls in the minimum between the upper and lower van Hove peaks.

Introduction

The ternary molybdenum chalcogenides, of composition MMo_6X_8 (where M = metal; X = S, Se, Te), sometimes called Chevrel phases,[1] are of special interest because they are high-temperature, strong-field superconductors in which the superconducting critical temperature can be used as a sensitive probe to monitor subtle effects due to small changes in chemical composition.[2] Two parameters have turned out to be particularly useful in mapping empirical correlation of the critical temperature, viz., the unit-cell volume and the number of donor electrons provided by the ternary element M. In the BCS theory of superconductivity,[3] the superconducting critical temperature T_c is given by

$$kT_c \approx \langle \hbar\omega \rangle \exp(-1/NV)$$

where $\langle\omega\rangle$ is the mean phonon frequency, N is the density of states at the Fermi level, and V is the electron–phonon coupling constant. For the homologous series of compounds MMo_6X_8, $\langle\omega\rangle$ and V can be crudely approximated as constant, in which case ln T_c would be expected to be a decreasing function of $1/N$. Thus, in the zeroth approximation, we find T_c increasing with an increase in the density of states at the Fermi level. The empirical correlations of T_c with unit-cell volume and with electron-donor character of M reflect this dependency of T_c on N. For quasi-free electrons the density of states is generally proportional to the volume in which the electrons are confined; the number of such electrons is controlled by the donor capability of individual atoms in contributing to the collective electronic states. Ideally, the density of states goes as the square root of the energy, so it would appear to be a simple matter to compute the density from the degree of band filling. In practice, the band shapes are quite complicated functions of the specific crystal symmetry, the number and character of orbitals available, the extent of orbital hybridization, and the degree of band filling.

Several attempts have been made to calculate the band structure of the Chevrel phases in the framework of various approximations. Andersen, Klose, and Nohl[4] used the linear muffin-tin orbital method in the atomic-sphere approximation; Mattheiss and Fong[5] used the tight-binding method with parameters derived from augmented plane waves; Bullett[6] used a localized-orbital method; Jarlborg and Freeman[7] did ab initio self-consistent linear muffin-tin orbital studies. All the treatments agree in their basic findings and attribute superconductivity to the high Mo d-band density of states at the Fermi level resulting from large charge transfer of Mo electrons to the chalcogens and from the ternary element M to the cluster Mo_6X_8.

The structure of MMo_6X_8, shown in Figure 1 in idealized form, consists of Mo_6X_8 clusters with the X atoms approximating a cube and the Mo atoms being slightly above the centers of the cube faces. Each cube is rotated approximately 25° about its body diagonal ($\bar{3}$ axis) so that the X of one cluster approaches and is bonded to a Mo of a neighboring cluster. The ternary M atoms, when large, sit on the $\bar{3}$ axis between the rotated cubic clusters and, when small, in a double belt of 12 tetrahedral sites disposed around the $\bar{3}$ axis. The materials can be indexed on the basis of either a hexagonal cell (c along $\bar{3}$ and a perpendicular to the $\bar{3}$ axis) or a rhombohedral cell (the rhombohedral angle α is generally within a few degrees of 90°).

Having recently studied[8] the pseudobinary system $YbMo_6S_8$–$YbMo_6Se_8$ in order to find out why, in the rare-earth Chevrel phases, the superconductivity of the ytterbium member is anomalously high in the sulfide series and anomalously low in the selenide series, we here extend our studies to the pseudobinary systems $YbMo_6S_8$–$LaMo_6S_8$, $YbMo_6Se_8$–$LaMo_6Se_8$, and $LaMo_6S_8$–$LaMo_6Se_8$. The goal was to separate out the effect of changing unit-cell volume from that of changing donor-electron density on the density-of-states function. The approach was to synthesize from ultrapure starting elements various mixed rare-earth molybdenum chalcogenides of well-defined stoichiometry, determine their crystallographic structure parameters, and measure their superconducting critical temperatures as a function of composition. Sulfur and selenium have practically the same electronegativities (2.5 and 2.4, respectively), but they differ in size (atomic radii 1.02 and 1.17 Å, respectively), so replacement of sulfur by selenium gives us a handle on changing unit-cell volume; La^{3+} and Yb^{2+} have about the same size (1.03 and 1.02 Å, respectively) and are both diamagnetic S_0 states, so that replacement of lanthanum by ytterbium enables us to manipulate the donor-electron density without changing the volume or introducing magnetic moments that would depress the superconductivity.

(1) Chevrel, M.; Sergent, M.; Prigent, J. *J. Solid State Chem.* **1971**, *3*, 515.
(2) For an excellent review of structural properties, see: Yvon K. *Curr. Top. Mater. Sci.* **1979**, *3*, 53. For physical properties, see: Fischer, Ø. *Appl. Phys.* **1978**, *16*, 1.
(3) Bardeen, J.; Cooper, L. N.; Schrieffer, J. R. *Phys. Rev.* **1957**, *106*, 162; **1957**, *108*, 1175.
(4) Andersen, O. K.; Klose, W.; Nohl, H. *Phys. Rev. B: Solid State* **1978**, *17*, 1209.
(5) Mattheiss, L. F.; Fong, C. Y. *Phys. Rev. B: Solid State* **1977**, *15*, 1760.
(6) Bullett, D. W. *Phys. Rev. Lett.* **1977**, *39*, 664.
(7) Jarlborg, T.; Freeman, A. J. *J. Magn. Magn. Mater.* **1980**, *15–18*, 1579; *Phys. Rev. Lett.* **1980**, *44*, 178.
(8) Tarascon, J. M.; Johnson, D. C.; Sienko, M. J. *Inorg. Chem.* **1982**, *21*, 1505.

0020-1669/83/1322-3769$01.50/0 © 1983 American Chemical Society

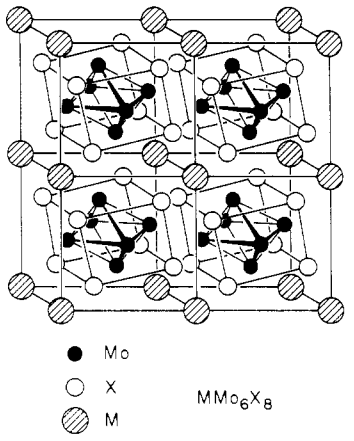

Figure 1. Idealized structure of MMo_6X_8.

Experimental Section

Sample Preparation. Starting materials were La (99.99%), Yb (99.99%), and Mo (99.95%), from United Mineral and Chemical Corp., and S and Se (99.9999%), from Atomergic Chemetals Corp. The Mo powder was reduced prior to use at 1000 °C under a flow of hydrogen and stored in a vacuum desiccator until needed.

Appropriate amounts of the elements to form 1-g samples of the mixed compounds, e.g. $Yb_{1-x}La_xMo_6S_8$ (x = 0–1, in steps of 0.1), were placed in previously degassed silica tubes, which were degassed again at 10^{-6} torr and sealed. All the tubes of a given series were placed together in a box furnace, the temperature of which was uniformly and slowly raised to 1050 °C over the course of 5 days. After 24 h at 1050 °C, the sample tubes were cooled in air and vigorously shaken so as to homogenize. They were immediately reheated to 1100 °C, kept there for 48 h, and then air-cooled. The samples were removed to a helium Dri-Lab where they were opened and thoroughly ground. After they were resealed in new degassed silica tubes, which were sealed in bigger ones, the samples were heated as previously described. The samples were then heated at 1220 °C for 96 h and finally air-cooled.

Powder X-ray Diffraction. X-day diffraction photographs were made by using a 114.6-mm diameter Debye–Scherrer camera with nickel-filtered Cu Kα radiation. Lines were indexed with the aid of a Fortran program that calculated the positions and intensities of possible reflections from available single-crystal data. A least-squares fit, with correction for absorption and camera-radius error, was performed by using all lines with $\theta(hkl) < 30°$ that could be indexed unambiguously. The procedure yields lattice parameters with errors of less than one part per thousand. All samples were single phase to X-ray analysis.

Superconducting Transition Determination. The transition to the superconducting state was monitored by using an ac mutual-inductance apparatus, which has been described elsewhere.[9] In this device, the detection system is a primary coil with two opposed external secondary coils wound symmetrically about it. The sample was placed in one of the secondary coils, and onset of superconductivity is signaled by an abrupt increase in magnetic shielding when the sample becomes perfectly diamagnetic. Temperature was measured by using a calibrated CryoCal germanium thermometer, which was checked against the boiling point of helium and the superconducting transition temperatures of lead and niobium. The T_c value was taken as the temperature at which the inductively measured transition was half-complete. The width of the transition is the temperature difference between the points where the transition is 10% and 90% complete.

Results and Discussion

Figures 2 and 3 show the X-ray data for the series of compounds $Yb_{1-x}La_xMo_6S_8$ and $Yb_{1-x}La_xMo_6Se_8$, respectively. For both series, there is a complete solid solution over the whole range from all ytterbium to all lanthanum. The hexagonal lattice parameters, a_H and c_H, change gradually (Figures 2a and 3a), but Vegard's law is not obeyed; c_H exhibits a positive deviation, and a_H shows a negative one. Similarly, for the rhombohedral lattice parameters, whereas a_R is almost precisely linear with x (Figures 2b and 3b), α_R shows negative deviations from Vegard's law (Figures 2c and 3c). Interestingly, the unit-cell volume, within the precision of the mea-

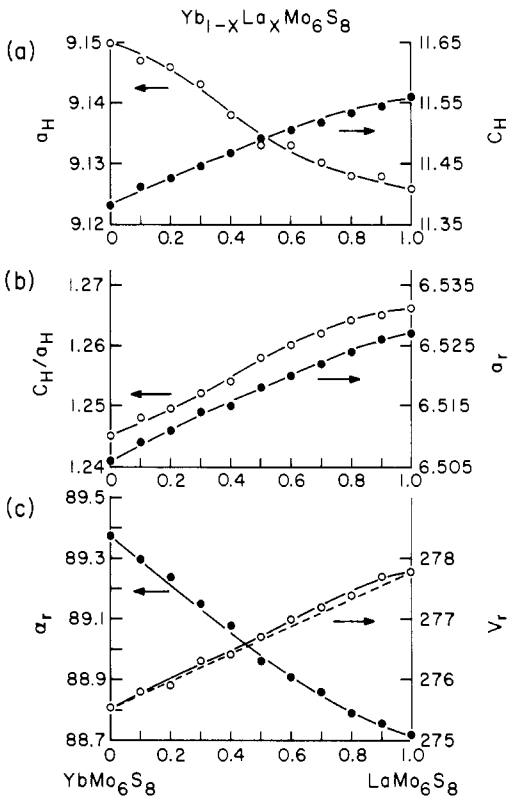

Figure 2. X-ray data for $Yb_{1-x}La_xMo_6S_8$. The parameters a_H and c_H are the axial lengths for hexagonal indexing; the parameters a_R and α_R are respectively the axial length and interaxial angle for rhombohedral indexing. V_R is the volume of the rhombohedral unit cell. The size of the data points exceeds the error in the fitted values.

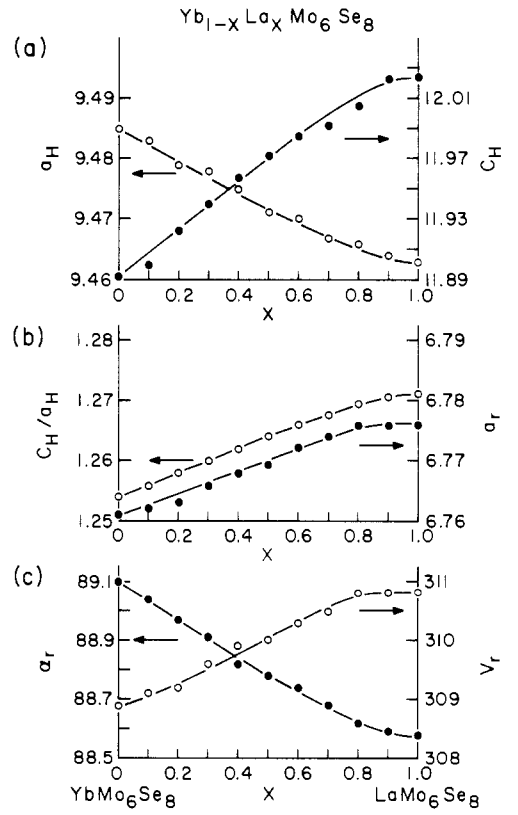

Figure 3. X-ray data for $Yb_{1-x}La_xMo_6Se_8$ (notation as in Figure 2).

(9) Fisher, W. G. Ph.D. Thesis, Cornell University, 1978.

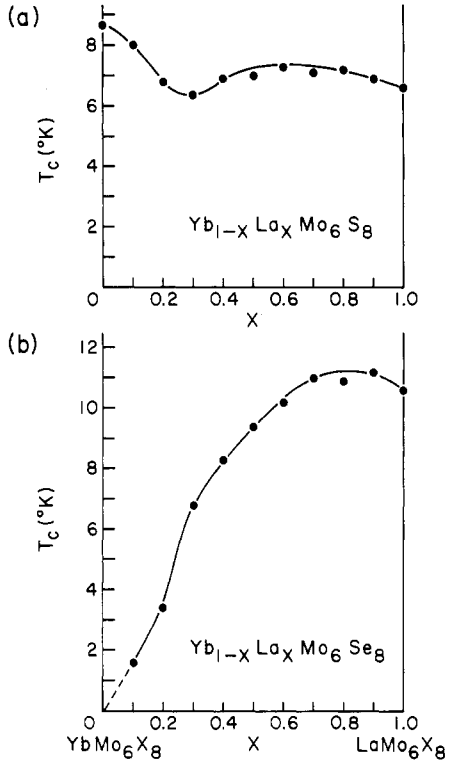

Figure 4. Superconducting critical temperature T_c vs. composition in the series (a) $Yb_{1-x}La_xMo_6S_8$ and (b) $Yb_{1-x}La_xMo_6Se_8$.

surements, appears to be linear with x, which suggests that the oxidation state of ytterbium remains constant along the series.

All of the compounds, except $YbMo_6Se_8$ ($x = 0$ in the series $Yb_{1-x}La_xMo_6Se_8$), turn out to be superconductors. The superconducting critical temperatures are shown in Figure 4. In the sulfide series, $Yb_{1-x}La_xMo_6S_8$, the first 20% of lanthanum substitution for ytterbium decreases the critical temperature but then T_c remains essentially constant. In the selenide series, $Yb_{1-x}La_xMo_6Se_8$, substitution of La for Yb causes T_c first to increase dramatically but then after about 70% replacement T_c again levels off. Magnetic data for the end members $YbMo_6S_8$ and $YbMo_6Se_8$ indicate that the ytterbium is practically all divalent;[8] measurements on $LaMo_6S_8$ and $LaMo_6Se_8$[10,11] show that lanthanum is trivalent. Thus, in the series $Yb_{1-x}La_xMo_6S_8$ and $Yb_{1-x}La_xMo_6Se_8$, as x increases there is progressive increase in the number of electrons transferred from the ternary element M to the cluster Mo_6X_8. The dramatic difference between sulfide and selenide series clearly implies that we are tracing out entirely different portions of the conduction-band density-of-states curve.

In the current model for the superconductivity of the Chevrel phases, the superconducting band is a narrow doubly degenerate E_g band primarily composed of Mo 4d orbitals [mainly of E_g ($x^2 - y^2$) character but also t_{1u} (xz, yz), t_{2g} (xz, yz), and t_{2u} ($x^2 - y^2$)] with some covalent mixing with the chalcogen p orbitals. If, as in first approximation, this band is assumed to be rigid, i.e., the shape of the $N(E)$ function does not change with change in chemical composition, then the value of $N(E)$ at the Fermi level is dependent only on the degree of band filling. In principle, the ternary element M could contribute four electrons to this E_g band. With M divalent, the band would be half-filled; with M trivalent, it would be three-fourths filled. However, this ignores the role of the p orbitals. In the sulfides, the p orbitals are quite low in energy. They act as

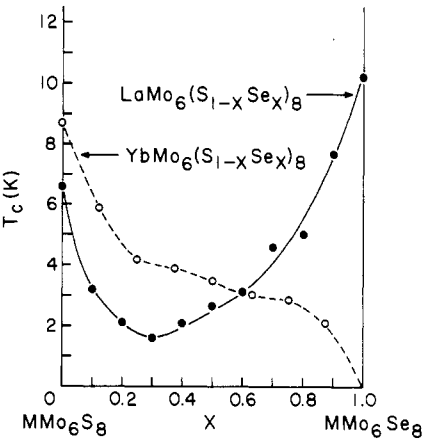

Figure 5. Effect of selenium-for-sulfur replacement on the superconducting critical temperature T_c in the system $LaMo_6S_8$–$LaMo_6Se_8$ as compared with the system $YbMo_6S_8$–$YbMo_6Se_8$.

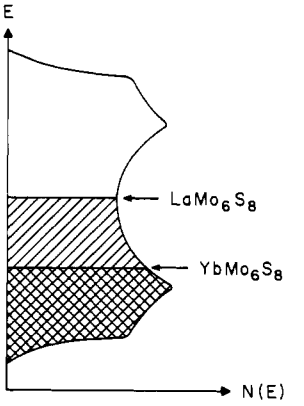

Figure 6. Schematic representation of probable band filling of the E_g band in the system $YbMo_6S_8$–$LaMo_6S_8$. Ordinate E is the energy in arbitrary units; abscissa $N(E)$ is the number of states per energy unit. Arrows indicate probable locations of Fermi levels.

deep traps, and the sulfur atoms almost appear as if they were 2– ions. In the selenides, on the other hand, the p orbitals lie higher; they tend to push electron density back on the molybdenum, and the selenium atoms appear more like 1.7– ions. This relative shifting of the chalcogen p band with respect to the Mo d band is what makes difficult an a priori calculation of the degree of filling of the E_g band. Not only do we have to distinguish the ternary element M as a two-electron or three-electron donor, but we need to recognize that going from sulfide to selenide also effectively increases electron donation to the E_g band, changing the degree of band filling.

In our previous study[8] of the $YbMo_6S_8$–$YbMo_6Se_8$ systems, we had looked directly at the effect on the superconductivity of replacing selenium for sulfur. The T_c drops more or less continuously from 8.65 K for $YbMo_6S_8$ to <1.5 K for $YbMo_6Se_8$. As part of the present investigation, we have also prepared the series $LaMo_6(S_{1-x}Se_x)_8$ to monitor the effect of selenium-for-sulfur replacement. As shown in Figure 5, the results are quite different. Unlike the monotonic drop in the ytterbium series, T_c in the lanthanum series passes through a minimum. The implication is that, with increasing band filling, the density of states in the lanthanum system first decreases and then increases whereas in the ytterbium system $N(E)$ falls continuously on a decreasing branch of the density-of-states curve.

Figure 6 shows schematically the probable band shape for the E_g band (from ref 4) and the probable location of the Fermi levels in $YbMo_6S_8$ and $LaMo_6S_8$, as deduced from the T_c vs. x curve for $Yb_{1-x}La_xMo_6S_8$ (Figure 4a). The unit cell volume in passing from $YbMo_6S_8$ to $LaMo_6S_8$ changes less

(10) Pelizzone, M.; Treyvaud, A.; Spitzli, P.; Fischer, Ø. *J. Low Temp. Phys.* **1977**, *29*, 453.
(11) Johnston, D. C.; Shelton, R. N. *J. Low Temp. Phys.* **1977**, *26*, 561.

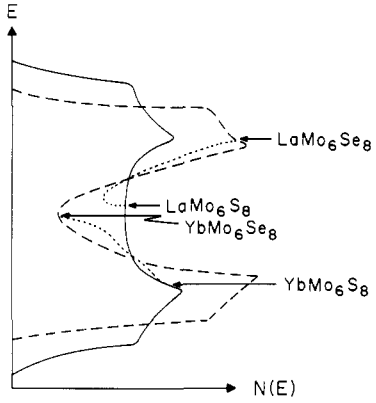

Figure 7. Probable density-of-states changes: dashed curve, selenides; solid curve, sulfides. The dotted traces indicate the observed $N(E)$ changes for $YbMo_6(S_{1-x}Se_x)_8$ and $LaMo_6(S_{1-x}Se_x)_8$. Arrowheads again indicate probable locations of Fermi levels.

than 1%, so the dominant change is the 50% increase in donated electrons. Higher energy states would need to be filled to accommodate electrons, but the crucial thing is that the uppermost-filled state would have to fill in a region of lower but not rapidly changing density of states $N(E)$ to agree with the observed drop and flattening out of the superconducting critical temperature.

Figure 7 shows how the band shape probably changes in going from sulfides to selenides. The solid curve (same as Figure 6) shows the band for the sulfides; the dashed curve represents the band for the selenides. Because the selenium atom is larger than the sulfur atom, there is an expansion in unit-cell volume. The molybdenum distances become greater, the orbital overlap is less, and the density of states increases. The bandwidth in the selenides is therefore appreciably narrower than in the sulfides. We have shown the baricenter of the two bands unchanged, but this is probably not the case, given the expansion of the unit cell and also the increased covalency in the selenides. Both influences probably act to lower the baricenter of the selenide band relative to that of the sulfide band.

We have placed the Fermi level for $LaMo_6Se_8$ just above the upper peak of the E_g band. That the Fermi level is near a van Hove singularity (maximum, minimum, or saddle point in the energy vs. wave vector curve) is clear from the magnetic susceptibility behavior.[11] The Pauli susceptibility, instead of being, as normal, independent of temperature, rises linearly with decreasing temperature, as was found in the $PbMo_6(S_{1-x}Se_x)_8$ system.[12] From Figure 4b, it is seen that the first bit of substitution of Yb for La in $LaMo_6Se_8$ first raises the T_c and then rapidly depresses it. This could correspond to scanning downward over the van Hove peak.

Assuming that Yb-for-La substitution does not change the band shape, but Se-for-S replacement narrows the band and increases the density of states at the two peaks, we can use Figure 7 to correlate schematically the observed changes in T_c with composition. To do this, we set up a three-dimensional space in which distance behind the plane of Figure 7 represents the percent of sulfur replaced. The solid curve, which we can take to be in the plane of the diagram, represents the sulfide system; the dashed curve, in some plane behind the diagram, represents the selenide system. Within the sulfide system, T_c changes in a high broad valley between two rather low peaks; in the selenide system, it changes in a narrow steep valley between two high peaks. As we go from $LaMo_6Se_8$ to $LaMo_6S_8$, we pass from near a peak of the narrow-valley system to the floor of the broad-valley system; in going from $YbMo_6Se_8$ to $YbMo_6S_8$, we pass from the bottom of the narrow-valley system to a shoulder of the broad-valley system. The dotted traces indicate the respective paths as derived from direct correlation of T_c with $N(E)$.

Unfortunately, this model is too simple for the $MMo_6S_{1-x}Se_x$ series. It puts all the burden for changing T_c on $N(E)$; composition-induced changes in lattice stiffness ($\hbar\omega$) and electron–phonon coupling (V), which could compensate for local details in the density-of-states structure, are ignored. Furthermore, the above analysis assumes a uniformly continuous change in Se-for-S replacement in the sense that site occupancy is assumed to be randomly statistical. Crystal structure data[12] strongly suggest that selenium-for-sulfur substitution first occurs on general-position chalcogen sites and then on special-position sites on the $\bar{3}$ axis. If so, then we might expect a discontinuity in the $N(E)$ vs. composition curve when six of the eight sulfur atoms have been replaced by selenium. The larger size of the selenium atom compared to that of sulfur would then make its effect felt first on the a parameter and subsequently on the c parameter. Increasing the a distance should have a larger effect on increasing the density of states than on increasing the c distance. Therefore, in passing from sulfide to selenide, the density of states should increase faster for the first six Se-for-S substitutions than for the last two. It must be noted, however, that site ordering probably has a smaller effect on the density of states than band narrowing, increasing covalence, or baricenter displacement. Still, it may explain some of the discrepancies in T_c reported in the literature for ostensibly identical preparations. It may be that annealing times and temperatures have to be carefully reproduced.

Acknowledgment. This research was sponsored by the Air Force Office of Scientific Research through Grant No. AFOSR 80-0009 and was supported in part by the National Science Foundation and the Materials Science Center at Cornell University.

(12) Delk, F. S., II; Sienko, M. J. *Inorg. Chem.* **1980**, *19*, 1352.